sustainability

MDPI

Article

Dispersal Characteristics and Pathways of Japanese Glass Eel in the East Asian Continental Shelf

Yu-San Han [1,*,†], Kuan-Mei Hsiung [2,3,†], Heng Zhang [4,*], Lai-Yin Chow [1], Wann-Nian Tzeng [1], Akira Shinoda [5], Tatsuki Yoshinaga [6], Sung-Pyo Hur [7], Sun-Do Hwang [8], Yoshiyuki Iizuka [9] and Shingo Kimura [2]

1 Institute of Fisheries Science, College of Life Science, National Taiwan University, Taipei 10617, Taiwan; yinlove6@gmail.com (L.-Y.C.); wnt@ntu.edu.tw (W.-N.T.)
2 Graduate School of Frontier Sciences, Atmosphere and Ocean Research Institute, University of Tokyo, Chiba 277-8564, Japan; km-hsiung@nenv.k.u-tokyo.ac.jp (K.-M.H.); s-kimura@aori.u-tokyo.ac.jp (S.K.)
3 Institute of Oceanography, Shanghai Jiao Tong University, Shanghai 200240, China; km-hsiung@sjtu.edu.cn
4 East China Sea Fisheries Research Institute, Chinese Academy of Fishery Sciences, Shanghai 200090, China
5 Department of Biology, Tokyo Medical University, Shinjuku, Tokyo 160-8402, Japan; shinoda@tokyo-med.ac.jp
6 School of Marine Biosciences, Kitasato University, Kanagawa 252-0373, Japan; yosinaga@kitasato-u.ac.jp
7 Jeju International Marine Science Research & Logistics Center, Korea Institute of Ocean Science & Technology, Jeju 63349, Korea; hursp@kiost.ac.kr
8 Korea Fisheries Resources Agency, Gunsan 54021, Korea; sdhwang@fira.or.kr
9 Institute of Earth Sciences, Academia Sinica, Taipei 11529, Taiwan; yiizuka@earth.sinica.edu.tw
* Correspondence: yshan@ntu.edu.tw (Y.-S.H.); zhangziqian0601@163.com (H.Z.); Tel.: +886-2-33663726 (Y.-S.H.); +86-13816338452 (H.Z.)
† Co-First authors. Tel.: +886-15721576334 (K.-M.H.)

Received: 12 March 2019; Accepted: 24 April 2019; Published: 4 May 2019

Abstract: The Japanese eel *Anguilla japonica* is an important aquaculture fish species in the East Asian countries of Japan, China, Korea, and Taiwan. All glass eel fry are captured from the wild and understanding the recruitment patterns of the glass eel is important. The larvae of *A. japonica* are passively transported to the East Asian Continental Shelf by the North Equatorial Current, the Kuroshio, the Kuroshio intrusion currents, and coastal currents. In each location, recruitment time is diverse: It is November in Taiwan and April in the Yalu River. How the glass eels reach recruitment areas remains poorly understood. Here, we combine information from larval ages based on otolith increments, simulated drifting paths on the East Asian Continental Shelf, and main fishing seasons in each location of East Asia. We identify five main recruitment blocks: (1) The main Kuroshio, (2) The Taiwan Strait Warm Current, (3) The Taiwan Warm Current, (4) The Yellow Sea Warm Current and (5) The branch of Yellow Sea Warm Current. The counted age of the glass eels is significantly underestimated for the later recruits, possibly due to the cessation of the otolith edge growth under low water temperatures. This study clarifies the eel's larval characteristics and transport mechanisms in the East Asia Continental Shelf, providing important information for its recruitment dynamics in the marine stage.

Keywords: *Anguilla japonica*; leptocephalus; glass eel; Kuroshio; North Equatorial Current (NEC); otolith daily increments

1. Introduction

The Japanese eel *Anguilla japonica* (Temminck & Schlegel) is a temperate catadromous fish mainly distributed in Taiwan, China, Korea, and Japan [1–3] and has been a commercially important freshwater

fish in East Asia. Large-scale commercial artificial propagation of the glass eel is still unavailable, and so the fry used in aquaculture can only be obtained by capture in estuarine and coastal waters during their upstream migration. Japanese eel resources have been declining significantly since the late 1970s [4–7]. The mean annual catch of adult wild Japanese eel in Japan has declined from approximately 3000 tons in the 1970s to 71 tons in 2017 [8]. In response to this resource crisis, the Japanese eel was listed as an "endangered" species in 2013 by the Ministry of the Environment, Government of Japan [9]. In 2014, it was listed in the IUCN Red List of Threatened Species as an "endangered" species [10,11] then in 2017, the Japanese eel was listed as a "critically endangered" species in the freshwater Red List by the Forest Bureau of Council of Agriculture, Taiwan [12]. A combination of factors has caused this decline, including habitat degradation [7,13,14], overfishing [15–17], and fluctuations in oceanic condition [6,18–22]. In 2007, the European eel *A. anguilla* was listed in Appendix II of the Convention on International Trade in Endangered Species of Wild Fauna and Flora (CITES) [23]. CITES imposes controls on the international trade of selected species. Since that time, the exploitation of the European eel resource has significantly declined [24]. The trade of both glass eel and adults of Japanese eel is active in China, Japan, Korea and Taiwan and would be greatly impacted if the Japanese eel were to be listed in Appendix II of CITES. To ensure the sustainability of the Japanese eel, Taiwan, China, Korea, and Japan signed a voluntary informal agreement to co-operate on the management of the Japanese eel in 2013. For sustainable use of this species, better understanding of its early life history is necessary.

The spawning area of the Japanese eel was discovered near 12°–16° N, 141°–142° E in the North Equatorial Current (NEC) about 3000 km away from its habitat in East Asia [25,26]. Mature eels mainly spawn between May and August during the new moon period [27–30]. The synchronized spawning behavior of *A. japonica* during the new moon may form a batch containing individuals of the same cohort, which is transported to the East Asian Continental Shelf, forming approximately monthly arrival waves [30]. After hatching, the larvae (leptocephali) passively drift from the spawning sites on the North Equatorial Current (NEC) and then the Kuroshio and its branch waters for 4–6 months before metamorphosing into glass eels and reaching the East Asian coasts [1,25,26,29,31]. Glass eels transform into a benthic sheltering behavior and actively swim toward nearby estuaries and rivers for growth [2,29,32].

The NEC bifurcates into the south-flowing Mindanao Current (MC) and the north-flowing Kuroshio at its westernmost boundary off the coast of the Philippines [33,34]. In winter, strong northeast winds push cold coastal waters southward, while the Kuroshio moves the offshore warm waters northward [35–38]. The warm and cold waters mix in the East Asian Continental Shelf and form complex offshore and coastal currents that are affected by factors such as local wind, water temperature and salinity, seabed topography and tides (see Ye for a general review) [39]. For example, Kuroshio bifurcates approximately 28° N south of Kyushu to form the Tsushima Current and the left branch of the Kuroshio moves onto the shelf as the Yellow Sea Warm Current (YSWC) [40,41] (Figure 1). The Taiwan Warm Current (TWC) flows northward from northeastern Taiwan into the coasts of Fujian and Zhejiang Provinces, China [29] (Figure 1). The intrusion of the Kuroshio in the central region of the Luzon Strait flows into northeast of the South China Sea, with some flowing directly into the Taiwan Strait as the Taiwan Strait Warm Current (TSWC) [42–44] (Figure 1). Due to a paucity of assimilation data for the offshore currents around the continental shelf, the detailed transport pathway of the eel larvae in the East Asian Continental Shelf remains poorly known.

According to a previous study, every East Asian location has a different recruitment time and main fishing season for the Japanese glass eel [31]. Its recruitment begins in early-to-middle November in Taiwan with the main fishing season occurring between December and January. The latest recruitments occur on the northeastern coasts of China (Yalu River) in April. The main fishing season between southern and northern East Asia has a maximum time lag up to five months [4,31]. In theory, the duration that larvae have drifted for is proportional to the number of the increment in the otolith [1]. The first larvae to arrive should have fewer increments than the last to arrive. However, an analysis of otolith increments suggested a less than two-month difference in the mean age between low and

high latitude samples [31]. These discrepancies are probably due to an underestimation of the otolith increments in the glass eel zone due to low water temperature [31,45]. If this is correct, then the later recruits should be the same, and age data alone may not be an appropriate method for investigating the dispersal time of glass eels. A combination analysis instead of the otolith increment counting may improve this shortcoming.

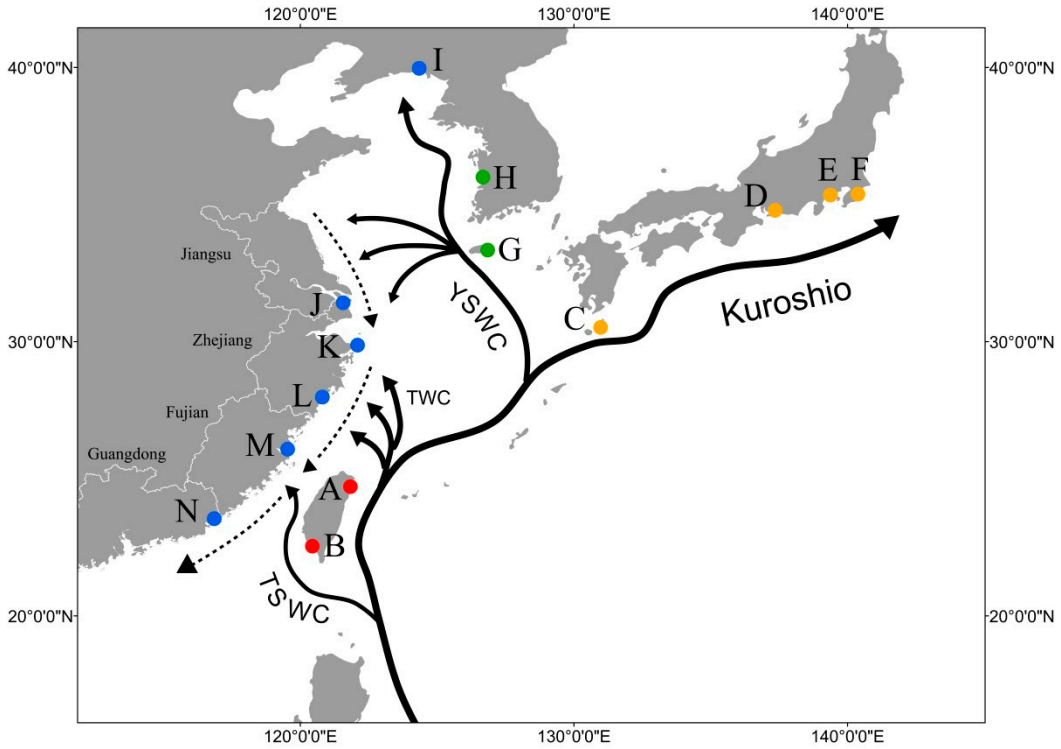

Figure 1. Sampling sites and oceanic currents in the East Asian Continental Shelf. (**A**) I-Lan; (**B**) Ping-Tung; (**C**) Tanegashima Island; (**D**) Mikawa Bay; (**E**) Sagami River; (**F**) Ichinomiya River; (**G**) Je-Ju Island; (**H**) Geum River; (**I**) Yalu River; (**J**) Shang-Hai; (**K**) Ning-Bo; (**L**) Wen-Zhou; (**M**) Min River; (**N**) Xiang-Shan. TWC: Taiwan Warm Current, YSWC: Yellow Sea Warm Current, TSWC: Taiwan Strait Warm Current.

Due to the fragmented knowledge for the dispersal dynamics of the Japanese eel larvae in the East Asian Continental Shelf, larger-scale sampling, combined with multiple evidence are necessary to clearly construct the early life characteristics, as well as the dispersal routes of the Japanese glass eel. Based on the meta-analysis of the otolith age of the glass eels from the East Asian samples, it was found that the variations in the otolith increments of glass eels counted by different laboratories were large [31], possibly due to system error in the otolith increment counting. Thus, recounting age data by the same laboratory would effectively eliminate system errors and substantially improve the power of the analysis. This study combines information from (1) the otolith age investigation of glass eel samples in the East Asia range, (2) the detailed fishing seasons and size of glass eel at each catching sites and (3), particle tracking to simulate the eel larval migration routes in Kuroshio and its branch waters to reconstruct the early life characteristics and detailed transportation dynamics of Japanese eel larvae in the East Asian Continental Shelf.

2. Materials and Methods

2.1. Sample Collection

The *A. japonica* glass eel specimens were collected at night during the fishing season using a hand-trawling net, a fyke net or a boat net. They were collected from I-Lan in November 2010

and December 2011, Ping-Tung in December 1992 and January 2003 [46], Shang-Hai in February 2017, Wen-Zhou in February 2017, Ning-Bo in February 1993 [47], the Min River in March 1993 and March 2010 [46], Xiang-Shan in February 2017, the Yalu River in April 1992 [46] and April 2017, Tanegashima Island in December 2016, Mikawa Bay in February 2002, the Sagami River in February 2017, the Ichinomiya River (Chiba) in January 1994 [46], Je-Ju Island in January 2017 and the Geum River in Korea in March 2017 (Figure 1). After collection, the captured glass eels were immediately preserved in 95% ethanol. The scanning electron microscope (SEM) images for glass eel samples collected from previous studies were recalculated for the increments. The specimens were measured to the nearest 0.1 mm total length (TL) and their pigmentation stages were observed following Tesch & White [2]. To reduce the potential counting error due to the long glass eel duration, only new arrival samples (in Stages V_A and V_B with the youngest age) in each site were selected for analysis.

2.2. Otolith Preparation and Daily Increment Analysis

The otolith preparation was based on Tzeng [47]. Briefly, sagittal otoliths, the largest of the three pairs of otoliths in the inner ear, were extracted from each individual, embedded in epoxy resin (EpoxiCure®, BUEHLER) mixed with epoxy harder (EpoxiCure®, BUEHLER) with a ratio of 5:1, ground and polished to the near core using a grinding machine (mateServe®3000, BUEHLER), etched with 0.05M HCL for 5 s. The otoliths were vacuum coated with Au in an ion-sputter for observation with a scanning electron microscope (JSM-6360LV, JEOL) which was equipped with an energy dispersive X-ray spectrometer (EDS: Oxford EDS: Xmax 80) in the laboratory at the Institute of Earth Science, Academia Sinica. The images were photographed at 300 times magnification of the actual size to observe the entire otolith, and at 2000 times magnification of the actual size for the observation of daily increment analysis.

SEM photographs, taken at a 2000 times magnification, were combined together and used for the observation of otolith microstructure and for counting the number of daily increments. The otolith increments from the first feeding check to the edge were counted on the photographs. The information included age at metamorphosis of the leptocephali (larval duration, LD) and age at capture (age). The ten days of the preleptocephalus stage, during which no otolith ring is formed [48] were added to the age. The early growth rate (ERG) was calculated as (TL-3 mm)/LD [49] because a mean length of 3 mm TL at hatching stage was obtained for artificial fertilization of *A. japonica* [50].

2.3. Estimating Real Age and Glass Eel Size in the East Asian Areas

The glass eel fishing seasons and average sizes (pieces per kilogram) in each area were collected from multiple sources including published papers, Japan Aquaculture Information News [51], China Eel Information News [52], and glass eel traders of Taiwan and China. The theoretical real age of *A. japonica* glass eels in each location was based on the arrival date of glass eels. Given that I-Lan of Taiwan is the first location to collect glass eels in East Asia, their I-Lan arrival date was used as the reference to calculate the time lag from the first recruitment date in Taiwan and other sampling sites. Based on data from the Taiwan Japanese Glass Eel Reporting System [53], the first arrival time of the Japanese glass eel in I-Lan of Taiwan usually begins in approximately middle November. The eels spawned around the new moon period, and therefore, the estimated theoretical age of glass eel in I-Lan would be approximately 170–180 days [30]. The arrival dates of the glass eels in other sampling sites were calculated based on the time differences between the main fishing time of I-Lan and that of the other sampling sites.

2.4. Circulation Model and Particle-Tracking Scheme for Simulation of Larval Drifting Time and Route between Spawning Area and Recruitment Sites

In this study, the Japan Costal Ocean Predictability Experiment 2 (JCOPE2) was used for the circulation model, which was constructed from the Princeton Ocean Model with a generalized coordinate system [54]. The JCOPE2 system assimilates the satellite-derived sea surface height and

SST data and in situ temperature and salinity to reproduce the ocean state as accurately as possible. The model domain of JCOPE2 contains the western North Pacific (10.5–62° N and 108–180° E), with a horizontal resolution of 1/12° (8–9 km) and 46 vertical layers [55]. The daily JCOPE2 reanalysis fields cover the period from January 1993 to the present [56]. The simulated trajectories of passive particles carried by JCOPE2 and observed trajectories have been compared [57], and the results showed a satisfactory performance of JCOPE2 in simulating the three-dimensional circulation across the western North Pacific Ocean.

A particle-tracking experiment was conducted to observe the distribution and transport process of the *A. japonica* larvae from the spawning area to their habitats along the East Asian coasts. A three-dimensional (3D) advection–diffusion scheme was used, as shown in Equations (1) and (2):

$$X_{t+1} = X_t + U\Delta t + S_x\Delta t + R_x \times (2K_h\Delta t)^{-\frac{1}{2}} \quad (1)$$

$$Y_{t+1} = Y_t + V\Delta t + S_y\Delta t + R_y \times (2K_h\Delta t)^{-\frac{1}{2}} \quad (2)$$

Here, X_t and Y_t represent the horizontal position of the particle associated with a random walk toward lower salinity mass at time t; U and V represent the eastward and northward current velocities, respectively; S_x and S_y are the eastward and northward swimming speeds respectively, of the eel juveniles and R_x and R_y are normal random numbers with expected values of 0 and standard deviations of 1, which is multiplied by the diffusion rate in order to make sure that each particle is randomly diffused but not directional swimming toward a fixed compass direction. For the particle diffusion, 1×10^2 m^2 s^{-1} was adopted as the horizontal eddy diffusivity (Kh) and the time step (Δt) was 1 h. According to previous studies, the body length of *A. japonica* is highly correlated with age (days) and demonstrates a linear relationship before metamorphosis into glass eels [25,58,59]. This study has established a growth model for the larvae (leptochepalus) and juveniles (glass eel) of this species to evaluate the swimming ability of *A. japonica*. This growth model set the expected metamorphosis timing of larvae (t_{meta}) to 115.2 ± 19.6 days and the expected maximum body length (TL_{max}) to 57.0 ± 2.6 mm [59] in order to construct a linear model to calculate body growth rate from hatching. The growth rate is based on Equation (3):

$$Growth = \frac{(TL_{max} - TL_0)}{t_{meta}} \quad (3)$$

where *Growth* represents the growth rate of Japanese eel larvae (mm day^{-1}) and TL_0 is the body length upon hatching (3 mm). After obtaining the growth rate, body length is calculated according to Equation (4):

$$\begin{cases} TL_t = TL_0 + Growth \times t, \ t \le t_{meta} \\ TL_t = TL_{max}, t > t_{meta} \end{cases} \quad (4)$$

where TL_t represents the body length of eel larvae or post-larval glass eels at time t (days), and we set conditions in which the eel larvae stop growing after they begin to metamorphose. It is known that Japanese eel larvae have poor swimming ability and thus we assumed that individuals are transported passively (0 TL s^{-1}) during the leptocephalus stage. However, the swimming ability increases when the eel larvae metamorphose into the glass eel. In these cases, the swimming speeds were set at 2 TL s^{-1} based on the previous study [60], which best reflects the field observation than other swimming speeds. Moreover, the swimming direction in our simulation is affected by salinity because a previous study reported that *A. anguilla* juveniles appear to prefer swimming toward lower-salinity water [61]. The vertical distribution in the simulation of this study was fixed at a depth of 150 m during the day (6 a.m. to 6 p.m.) and 50 m at night (6 p.m. to 6 a.m.) [22].

Previous studies have shown that the spawning season of *A. japonica* occurs predominantly from May to August [47,62,63], and the migration period estimated from observations is approximately six to eight months [64]. In this study, we investigated the distribution of the *A. japonica* larvae among the

East Asian coasts. From 1993 to 2018, 10,000 particles were released to simulate the eel larvae on two model dates, July 1, and August 1, and tracked for 240 days (eight months). The start location in the numerical simulations was set at latitude 14.5° N and longitude 142° E. At the end of the eight-month simulation, the location of each particle was categorized as follows: (i) Recruited to Chiba prefecture, Japan (33–33.5° N, 140–140.5° E); (ii) recruited to the coast of Tanegashima Island, Japan (30–31° N, 130–132° E); (iii) recruited to west of Je-Ju Island, Korea (34–35° N, 124.5-125.5° E); (iv) recruited to eastern Yangtze River, China (30–31° N, 123.5–124.5° E); (v) recruited to northeastern Taiwan (crossed 24–26° N, 122–123° E); or (vi) recruited to southwestern Taiwan (crossed 21–22° N, 120–122° E).

2.5. Data Analysis

Total length, larval duration, age, and early growth rate data for each location were checked first by Kolmogorov-Smirnov tests. All data set were fitted to the normal distribution. Thus, differences in the mean total length, larval duration, age, and early growth rate among sites were tested using the One-Way Analysis of Variance (ANOVA) followed by Tukey's honestly significant difference (HSD) multiple-comparison test. For the statistical analysis, the SPSS (ver. 16, IBM, NY USA) software was used. Differences were considered significant at $p < 0.05$. Linear regression analyses were tested for LD and total length, and for LD and early growth rate.

3. Results

3.1. The Mean Total Length, Body Weight, Larval Duration and Counted Ages of Glass Eels at Sampling Sites

The glass eel samples from I-Lan, Ping-Tung, Yalu-River, and Min-River were composed of samples from different years. However, there were no significant differences between the mean total length, body weight, larval duration and counted ages in each location ($p > 0.05$ for all). Therefore, the different batches of samples from each site were pooled together for analysis. The mean total length of glass eels ranged from 55.1 to 56.8 mm, with no significant differences found among sampling sites ($F = 1.396$, d.f. $= 13$, $p = 0.164$) (Table 1). The mean body weight was largest (5000–5500 pieces per kg) for glass eels from Taiwan and southern Japan, with 5500–6000 pieces per kg from middle and eastern Japan and the Min River, 6000–7000 pieces per kg from Je-Ju Island and central and southern China, and the smallest was 8000–9000 pieces per kg from the Yalu River (Table 2). The mean larval duration of glass eels ranged from 139.4 to 182.0 days, with significant differences found among sampling sites ($F = 43.038$, d.f. $= 13$, $p < 0.001$) (Table 1). I-Lan and Ping-Tung of Taiwan had the lowest mean increments and Yalu River of China had the largest. The number of increments trended upwards along the larvae's expected drifting paths. Significant differences were found between Yalu River and the other 15 sample sites and between the samples from Taiwan and other sites (Figure 2). The mean counted ages of glass eels ranged from 188.6 to 241.8 day, with significant differences found among sampling sites ($F = 37.162$, d.f. $= 13$, $p < 0.001$) (Table 1).

Table 1. Sampling location, time, sample number (N), mean total length (TL), mean larval duration (LD), mean age, and mean early growth rate (EGR) of *A. japonica* in this study.

County	Sampling Sites (Code)	Sampling Time	N	TL * (mm)	LD * (day)	Total Age * (day)	EGR * (mm/day)
Taiwan	I-Lan (A)	November 2010/December 2011	26	55.7 ± 2.6 (51.5–61.0)	140.1 ± 5.8 ^{a} (132–155)	188.6 ± 9.3 ^{a} (172–204)	0.38 ± 0.02 ^{e} (0.31–0.41)
Taiwan	Ping-Tung (B)	December 1992/January 2003	29	56.7 ± 2.1 (52.8–61.1)	139.4 ± 8.7 ^{a} (125–157)	190.4 ± 12.4 ^{a} (154–212)	0.39 ± 0.03 ^{e} (0.34–0.44)
Japan	Tanegashima Island (C)	December 2016	17	56.8 ± 1.7 (54.0–61.0)	154.1 ± 4.9 ^{bc} (147–164)	207.7 ± 6.9 ^{b} (197–223)	0.35 ± 0.02 ^{d} (0.32–0.39)
Japan	Mikawa Bay (D)	February 2002	14	56.8 ± 2.1 (54.0–60.5)	156.6 ± 6.4 ^{bcd} (143–166)	209.0 ± 6.2 ^{b} (194–214)	0.34 ± 0.02 ^{cd} (0.31–0.39)
Japan	Sagami River (E)	February 2017	11	55.1 ± 2.9 (50.0–59.0)	161.4 ± 4.4 ^{bcd} (155–167)	215.4 ± 6.5 ^{bc} (208–225)	0.32 ± 0.02 ^{bcd} (0.29–0.36)
Japan	Ichinomiya River (F)	January 1994	8	56.1 ± 1.4 (54.0–58.0)	163.8 ± 4.5 ^{cd} (155–170)	216.7 ± 5.3 ^{bc} (209–223)	0.32 ± 0.01 ^{bcd} (0.31–0.34)
Korea	Je-Ju Island (G)	January 2017	11	56.6 ± 1.5 (53.5–59.5)	153.4 ± 4.4 ^{b} (145–159)	211.5 ± 4.9 ^{bc} (203–220)	0.35 ± 0.01 ^{d} (0.33–0.38)
Korea	Geum River (H)	March 2017	10	56.4 ± 1.7 (54.0–59.5)	173.7 ± 6.1 ^{e} (165–184)	241.8 ± 7.0 ^{d} (233–255)	0.31 ± 0.02 ^{ab} (0.28–0.33)
China	Yalu River (I)	April 1992/April 2017	22	56.3 ± 2.1 (52.5–61.0)	182.0 ± 8.3 ^{f} (164–195)	240.0 ± 11.2 ^{d} (213–260)	0.29 ± 0.02 ^{a} (0.27–0.33)
China	Shang-Hai (J)	February 2017	12	55.7 ± 1.9 (54.0–60.2)	166.0 ± 11.1 ^{de} (152–188)	223.2 ± 19.4 ^{c} (199–263)	0.32 ± 0.02 ^{abc} (0.27–0.35)
China	Ning-Bo (K)	March 1993	10	55.9 ± 1.9 (51.5–58.5)	157.3 ± 6.7 ^{bcd} (150–169)	209.8 ± 8.0 ^{bc} (199–220)	0.34 ± 0.02 ^{cd} (0.29–0.36)
China	Wen-Zhou (L)	February 2017	14	55.1 ± 1.3 (52.0–57.0)	158.7 ± 11.3^{bcd} (134–172)	215.4 ± 13.9 ^{bc} (186–234)	0.33 ± 0.03 ^{bcd} (0.30–0.40)
China	Min River (M)	February 1993/March 2010	15	55.6 ± 1.6 (51.6–58.0)	157.2 ± 9.4^{bcd} (145–177)	206.1 ± 10.9 ^{b} (192–220)	0.34 ± 0.03 ^{bcd} (0.29–0.37)
China	Xiang-Shan (N)	February 2017	12	55.0 ± 2.8 (51.0–62.0)	153.2 ± 11.6 ^{b} (134–167)	209.4 ± 14.3 ^{b} (185–228)	0.34 ± 0.03 ^{cd} (0.31–0.41)

* Unit: Mean ± SD; parenthesis: range; different letters beside Mean ± SD Different letters represent significant difference, $p < 0.05$.

Table 2. The estimated age, counted otolith age, time lag and body weight of Japanese glass eels in each location.

Sampling Sites (Code)	Estimated Age (day)	Counted Otolith Age * (day)	Time Difference (day)	Body Weight (Pieces per Kg)
I-Lan (A)	180	188.6 ± 9.3	0–10	5000–5500
Ping-Tung (B)	190	190.4 ± 12.4	0–10	5000–5500
Tanegashima Island (C)	200	207.7 ± 6.9	0–10	5000–5500
Mikawa Bay (D)	210	209.0 ± 6.2	0–10	5500–6000
Min River (M)	210	206.1 ± 10.9	0–10	5500–6000
Sagami River (E)	220	215.4 ± 6.5	0–10	5500–6000
Ichinomiya River (F)	220	216.7 ± 5.3	0–10	5500–6000
Wen-Zhou (L)	220	215.4 ± 13.9	0–10	6000–6500
Xiang-Shan (N)	220	209.4 ± 14.3	10–20	6500–7000
Je-Ju Island (G)	220	211.5 ± 4.9	0–10	6000–6500
Shang-Hai (J)	260	223.2 ± 19.4	30–40	6500–7000
Ning-Bo (K)	260	209.8 ± 8.0	50–60	6500–7000
Geum River (H)	270	241.8 ± 7.0	20–30	7000–7500
Yalu River (I)	330	240.0 ± 11.2	90–100	8000–9000

* Unit: Mean ± SD.

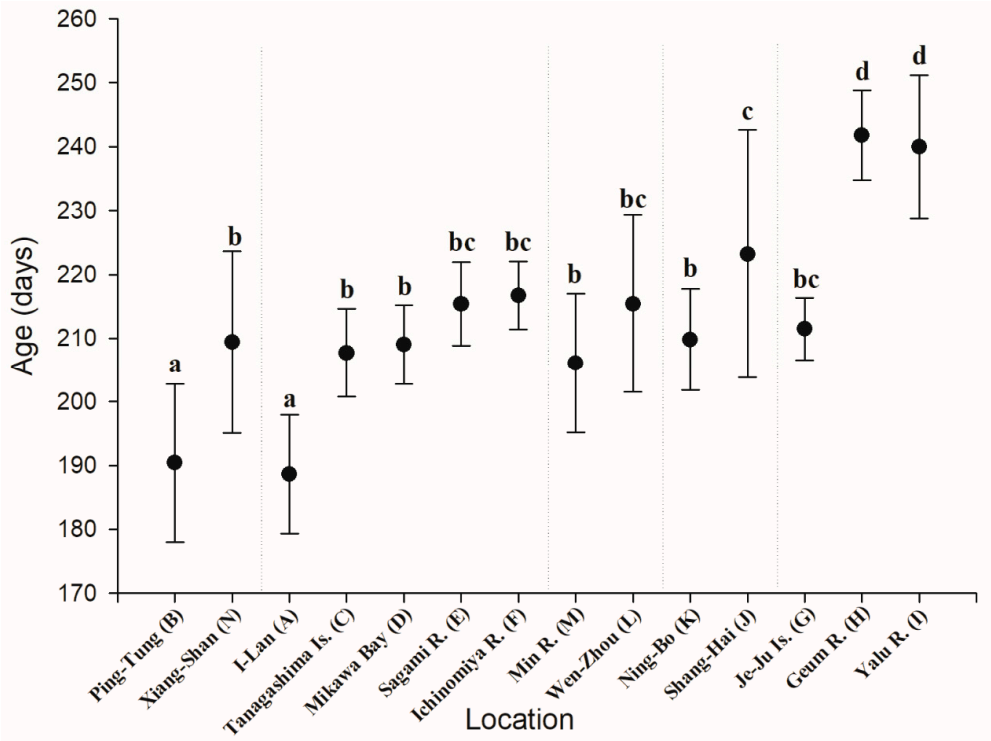

Figure 2. Comparison of the age of Japanese glass eel among Taiwan, Japan, Korea, and China. Different letters represent significant difference, $p < 0.05$.

3.2. The Estimated Real Age of Glass Eels on Sampling Sites

The glass eel recruitment in East Asia first begins in early-to-middle November in Taiwan, with the main fishing season occurring between December and January [31]. Three to four weeks later, the recruitment occurs in the Pacific coast of southern Japan (Kyushu) and the northern Fujian Provinces of China (around Xiapu), with the main fishing season between January and February. Soon after, the southern Zhe-Jiang and Fujian and northern Guang-Dong Provinces of China, Jeju Island of Korea, and Pacific coast of central and east Japan start their main fishing seasons between January and March. From February to April, the recruitments occur in the Jiangsu Province of China, mainly around the

Yangtse River estuary, northern Zhe-Jiang around Ning-Bo and the southern coasts of Korea. In the northern Jiangsu Province of China and the west coasts of Korea, the main fishing seasons are mainly between March and May. The latest recruitments occur at the northwestern coasts of Korea and Yalu River between April and June [31]. By combining multiple information sources, the theoretical real age of *A. japonica* glass eels in each location was estimated based on the time differences between the main fishing time of I-Lan and those of other sampling sites (Table 2).

The time lags between theoretical ages and mean counted otolith ages of glass eels ranged from 0 to 100 day (Table 2). In early recruitment sites, the estimated real age and mean counted otolith age were close, with time differences within 10 days. However, the time differences in later recruitment sites were between 20–30 days in the Geum River, 30–40 days in Shang-Hai, and 50–60 days in Ning-Bo. In the Yalu River, they were as high as between 90–100 days (Table 2).

3.3. The Relationship between Mean Larval Duration and Total Length/Early Growth Rate

The linear regression analysis revealed that the mean LD and TL of *A. japonica* showed no significant correlation ($R^2 = 0.014$, $p = 0.057$) (Figure 3). In contrast, the mean early growth rate of glass eels ranged from 0.29 to 0.39 mm/day (Table 1), with significant differences found among sampling sites ($F = 29.941$, d.f. $= 13$, $p < 0.001$). The regression analysis showed that the mean LD and EGR of larval *A. japonica* had a strong negative correlation ($R^2 = 0.861$, $p < 0.001$) (Figure 4).

3.4. The Simulated Dispersal Pathways and Time of Japanese Glass Eel from Spawning Area to Sampling Sites in the East Asian Continental Shelf

For the 240-day simulation, the transport process of the *A. japonica* larvae from the spawning areas to the habitats along the East Asian coasts was mainly along five routes (Figure 5). These were, i & ii: Main Kuroshio pathway in Tanegashima Island (206.6 ± 17.5 days) and Chiba (223.3 ± 12.0 days); iii: Branch waters of YSWC in west Je-Ju Island (227.8 ± 15.9 days); iv: Branch waters of YSWC in east Yangtze River (220.2 ± 10.2 days); v: TWC in northeastern Taiwan (192.0 ± 20.5 days); vi: TSWC in southwestern Taiwan (182.1 ± 23.8 days) (Table 3).

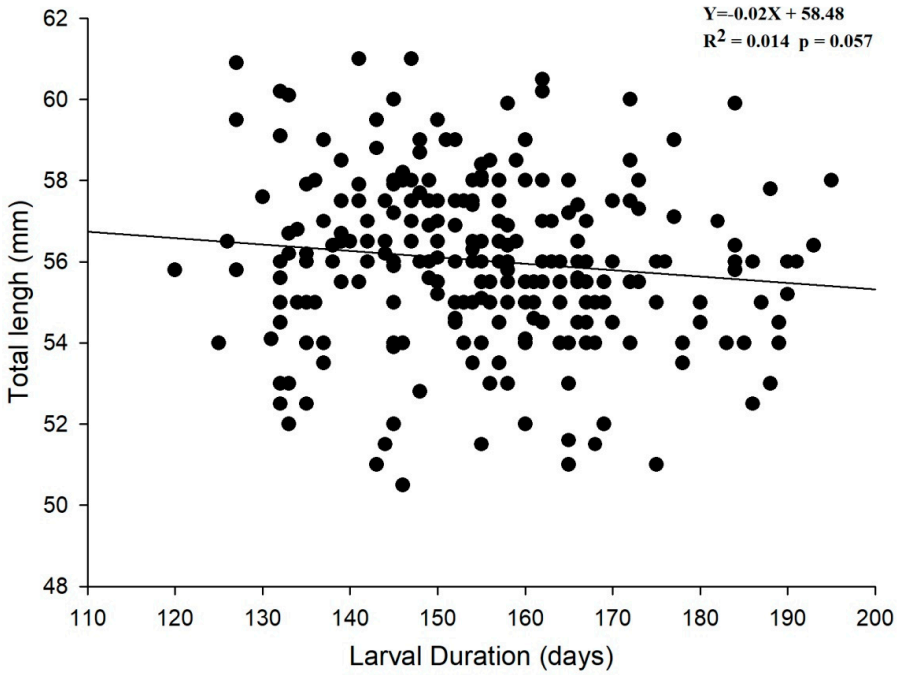

Figure 3. The regression of total length on larval duration of the Japanese glass eel ($n = 211$).

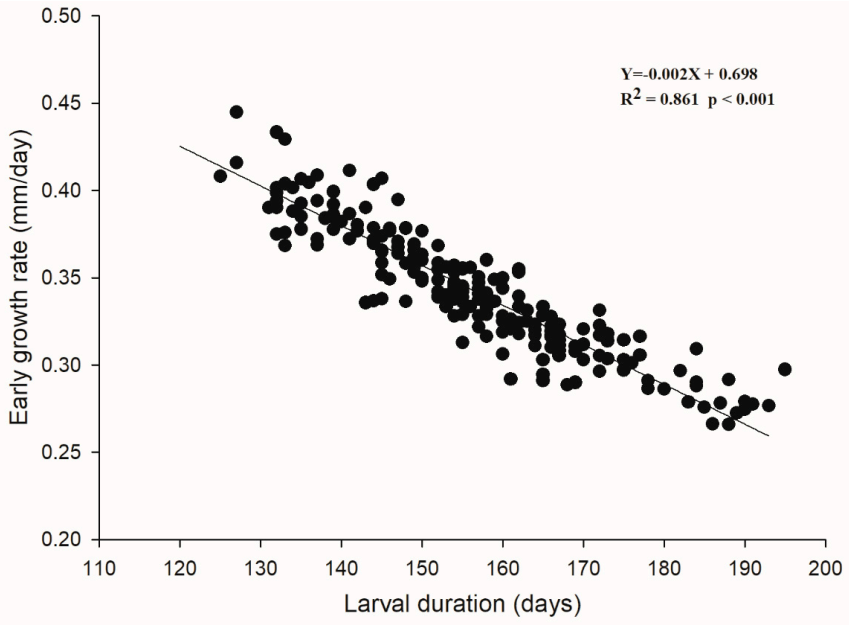

Figure 4. The regression of early growth rate on larval duration of Japanese glass eel (n = 211).

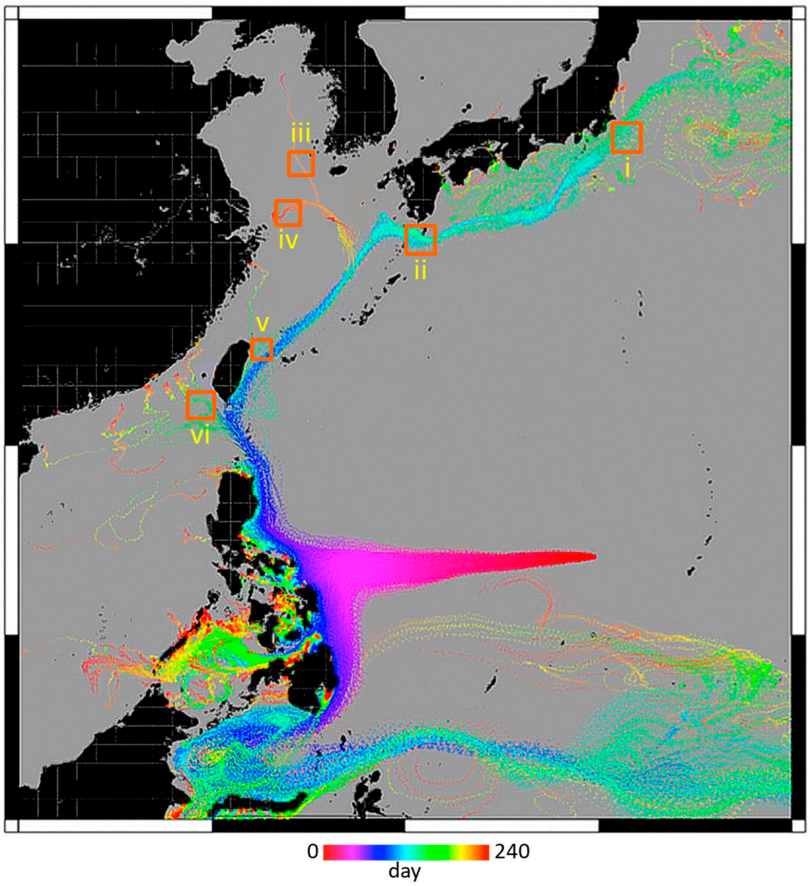

Figure 5. The simulated transport pathways and times of larval Japanese eel from spawning site to East Asia continental shelf. (i) recruited to Chiba prefecture, Japan (i.e., 33–33.5° N, 140–140.5° E); (ii) recruited to the coast of Tanegashima Island, Japan (i.e., 30–31° N, 130–132° E); (iii) recruited to west of Je-Ju Island, Korea (i.e., 34–35° N, 124.5-125.5° E); (iv) recruited to eastern Yangtze River, China (i.e., 30–31° N, 123.5–124.5° E); (v) recruited to northeastern Taiwan (i.e., crossed 24–26° N, 122–123° E); or (vi) recruited to southwestern Taiwan (i.e., crossed 21–22° N, 120–122° E).

Table 3. The simulated dispersal pathways and time of Japanese glass eel from spawning area to sampling sites in East Asian Continental Shelf.

Location	Geographic Coordinate	Duration (day) *
i: Chiba prefecture, Japan	33–33.5° N, 140–140.5° E	223.3 ± 12.0
ii: Tanegashima Island, Japan	30–31° N, 130–132° E	206.7 ± 17.5
iii: West of Je-Ju Island, Korea	34–35° N, 124.5–125.5° E	227.8 ± 15.9
iv: Eastern Yangtze River, China	30–31° N, 123.5–124.5° E	220.2 ± 10.2
v: Northwestern Taiwan	24–26° N, 122–123° E	192.0 ± 20.5
vi: Southwestern Taiwan	21–22° N, 120–122° E	182.1 ± 23.8

* Unit: Mean ± SD.

4. Discussion

4.1. The Total Length Variation of A. japonica at Different Sites

The mean total length of *A. japonica* collected from the 14 estuaries ranged from 55.1 to 56.8 mm. This result was consistent with the mean total length among *A. japonica* glass eels reported in previous studies [1,65]. The mean total lengths of *A. japonica* were not statistically different among the 14 sampling sites (Table 1), and there were no significant correlations between LD and TL (Figure 3). This infers that the metamorphosis of *Anguilla leptocephali* may be TL-dependent but not LD-dependent, which occurs when the TL reaches the maximum of leptocephalus size. Previous studies have suggested that the *A. japonica* leptocephali metamorphosed until the TL reached above 55 mm [25]. The TL-dependent metamorphosis may be because the energy stored by the leptocephali is required for the metamorphosis and metabolism of the subsequent glass eel stage. All anguillid and other leptocephali species have laterally compressed bodies that contain transparent energy-storage compounds, glycosaminoglycan (GAG), and lipids in their body, which are used to overcome starvation during metamorphosis [66,67]. Furthermore, glass eels of early recruitment (with lower LD and age) have higher growth rates than those of later recruitment (with lower LD and age) (Table 1, Figure 4). It is suggested that the age of glass eels upon arrival at the estuary was susceptible to larval growth rate, and this was supported by Tzeng [47] who found that the time taken for migration from the oceanic spawning ground to the estuary was shorter for the fast-growing larvae than for the slow-growing larvae. Therefore, the fast growing larvae takes a shorter time to reach a fixed maximum size, and thus metamorphose into glass eels at an earlier age and enter nearby estuaries and rivers in southern areas of East Asia. In contrast, the slow growing larvae take longer to reach a fixed maximum size, and thus metamorphose into glass eels at a later age and enter nearby estuaries and rivers in northern areas of East Asia.

4.2. The Under-Estimated Age of A. japonica Glass Eel in Later Recruits

A previous study indicated that the age composition of glass eel arrival batches in the three consecutive year classes in I-Lan of Taiwan showed comparable differences in the mean ages [30]. In the present study, the glass eel samples from I-Lan, Ping-Tung, Yalu-River, and Min-River composed of samples from different years. However, there were no significant differences between the mean total length and ages in each location, suggesting the generally stable age variations among year class samples. The recruitment season generally starts in I-Lan, Taiwan in November and in Yalu River, China in April of the following year, with a time lag of about 150 days. Increments in the otolith show, however, only an approximately 50-day difference in the mean otolith counted age between the I-Lan and Yalu River samples, which is considerably less than the expected recruitment time difference. Furthermore, the mean counted age of glass eels from some sampling sites was less than the theoretical age (Table 2). The later the fishing season of glass eels starts, the higher the age difference that would occur. Therefore, the true age of glass eels appears to be under-estimated for later recruits. After the larvae metamorphosed into glass eels, the otolith increments were deposited at the outermost part of the otolith, known as the glass eel zone. Previous studies found no discernible increments in this

part [63,68]. Furthermore, the otolith growth in glass eels was found to cease at between 10 °C and 15 °C [69,70]. Starvation [71], and possible re-absorption of marginal otoliths [45] may also contribute to the underestimation of increments in the outer part of the otolith of the glass eel. Furthermore, the back-calculated timing of spawning by otolith increments does not fit well with field observations of the spawning period as well as the spawning times estimated from leptocephalus samples [31]. This apparent mismatch has also been reported for the American eel (*A. rostrata*) with moderate discrepancy and European eel (*A. anguilla*) with large discrepancy [63,72]. The discrepancies are probably due to the methodological artefacts such as the resolution limit of microscopy [72]. The underestimation of the otolith increments in the glass eel zone would occur when the otolith growth rate is low, particularly for samples from high-latitude regions.

The spawning dates calculated from otolith increments of glass eels in Taiwan and Japan occur between May and August, which agree with the observed spawning periods. Since the leptocephali that metamorphose near the coastal waters of Taiwan and Japan could quickly approach estuaries due to the suitable migration temperature, the estimated glass eel age at these sites does not show underestimation. In contrast, the later recruits of glass eels from high latitude sites (northern China and Korea), with a longer glass eel stage due to the low water temperature in the winter [31], may have significantly underestimated post-leptocephalus duration, which has given rise to a marked inconsistency between counted age and real age.

4.3. The Metamorphosing Location of Japanese Eel Larvae in East Asia Continental Shelf

The mean larval duration of glass eels from Taiwan was approximately 140 days, whereas those from China, Japan, and Korea were approximately 153–182 days, meaning a difference of 13–42 days. This suggests that most leptocephali may metamorphose during their transport from Taiwan to Japan along Kuroshio [1], and some of them may metamorphose in the branched currents of the Kuroshio. Field studies support that the leptocephalus metamorphoses into the glass eel either along the Kuroshio between Taiwan and Japan [61], or through the mesoscale eddies to the east of Taiwan [65,71,73]. Although no metamorphosing leptocephali have as yet been found in the field investigation in the continental shelf, it is very possible that some leptocephalus may metamorphose into glass eels at the early time in the branched currents of the Kuroshio, and keep approaching the coasts by the glass eel stage. Interestingly, the mean body weight was found largest (5000–5500 pieces per kg) for glass eels from Taiwan and smallest (8000–9000 pieces per kg) for glass eels from the Yalu River (Table 2). The later recruits were of smaller body weights. This may reflect starvation during their movement in the seawater, or wintering at low temperatures for a period of time [31]. More field surveys in the East Asian continental shelf are necessary to further clarify the migratory characteristics of the leptocephalus and glass eel.

4.4. The Possible Dispersal Pathways of Japanese Eel Larvae Along East Asia Continental Shelf

Based on of the synthesized information from (1) particle tracking test to simulate the eel larval migration routes in Kuroshio, its branch waters and coastal currents, (2) the arrival time and size of glass eels at each sites and (3), the otolith age determination of glass eel samples, the detailed transportation pathways of the *A. japonica* larvae in the East Asian Continental Shelf could be constructed. In the Kuroshio pathway, the theoretical and simulated ages of glass eels in I-Lan were close. Based on the speed of Kuroshio (around 77–116 km/d) [1] and the difference in transported distance of glass eels between I-Lan and Tanegashima Island (1630 km), Mikawa Bay (2330 km), the Sagami River (2530 km), and the Ichinomiya River (2630 km), the expected differences in mean age of glass eels between I-Lan and Tanegashima Island, Mikawa Bay, Sagami River and Ichinomiya River should range between 14–21, 20–30, 22–33, and 23–34 days more than those in I-Lan, respectively. The age differences in glass eels between Taiwan and the sampling sites in Japan matched the expected differences (Table 2). Furthermore, the tracer simulation test suggested that Japanese eel larvae migrating from the spawning ground to Tanegashima Island and Chiba take approximately 206.6 ± 17.5 days and 223.3 ± 12.0 days,

respectively (Table 3). This corresponds with the estimated real age of the glass eel samples (Table 2). Taken together, the mean age of glass eels shows an increasing trend from I-Lan to Ichinomiya River (Figure 2), suggesting that the primary Kuroshio transports glass eels from Taiwan to Japan in a single direction. According to the long-term statistics of the Japan Aquaculture Information News, the average recruitment abundances of the Japanese glass eel in China, Japan, Taiwan, and Korea are 50–60%, 30–40%, 5–10%, 5–10%, respectively. In Japan, more than 90% of glass eels are caught along the Pacific coast, meaning that approximately one-third of all Japanese glass eels are transported by the primary Kuroshio pathway each year.

In the Taiwan Strait Warm Current pathway, the tracer simulation test suggested that Japanese eel larvae migrating from the spawning ground to southwestern Taiwan Island takes approximately 182.1 ± 23.8 days (Table 3), which matches the estimated real age of the glass eel samples in Ping-Tung (190.4 ± 12.4 days). The estimated real age of glass eels in Xiang-Shan should be 30 days more than that of Ping-Tung (Table 2). The supposed migratory path from Ping-Tung to Fujian was approximately 320 km in distance by TSWC, and around 220 km from Fujian to Xiang-Shan by the coastal current (Figure 1). Based on the velocity of the Taiwan Strait Warm Current, which ranged from 1.1 to 1.6 km/h and the East China Sea Coastal Current (0.9 km/h) [39], the expected time difference in the mean age of glass eels between Ping-Tung and Xiang-Shan was 19–22 days, which generally corresponds with the estimated real age difference between these two sites (30 days). However, the mean recruitment time difference of glass eels between Ping-Tung and Xiang-Shan was 19 days only, suggesting that the otolith counted ages of glass eel samples from Xiang-Shan are likely to be underestimated for around 10 days.

In the Taiwan Warm Current pathway, the tracer simulation test suggested that Japanese eel larvae migrating from spawning grounds to northeastern Taiwan Island takes around 192.0 ± 20.5 days (Table 3), which generally matched the estimated and counted mean ages of glass eels in I-Lan. The estimated real age of glass eels in Min-River and Wen-Zhou should be 20 and 30 days more than that of I-Lan, respectively (Table 2). The mean counted otolith ages of glass eels in Min-River and Wen-Zhou were 17.5 and 26.8 days higher than those of glass eels in I-Lan, respectively (Table 2), which correspond with the expected recruitment time differences. The shortest transported distances of glass eels between I-Lan, Min-River and Wen-Zhou along the TWC were around 330 and 380 km, respectively (Figure 1). Based on the speed of TWC (0.97–1.87 km/h) [39], if eel larvae were transported by TWC from I-Lan to Min-River and Wen-Zhou by the shortest paths, about 7–15 and 8–16 more days were needed, respectively. The estimated real mean age for glass eels in Min-River and Wen-Zhou were slightly higher than the estimated time, suggesting that glass eels may disperse by a curved path or partly by the coastal currents. In China, northern Fujian was the first recruitment place of the Japanese glass eel, suggesting that the TWC may transport glass eels from I-Lan to northern Fujian and southern Zhejiang by TWC, followed by the ECSCC to disperse glass eels southwards.

In the Yellow Sea Warm Current pathway, the tracer simulation test suggested that Japanese eel larvae migrating from spawning grounds to west Je-Ju Island takes approximately 227.8 ± 15.9 days (Table 3). This corresponds with the estimated and counted mean ages of glass eels in Je-Ju Island (Table 2). If larvae from I-Lan were transported to Je-Ju Island by the Kuroshio followed by the YSWC, the transport distance was about 1460 km. Based on the speed of Kuroshio and YSWC (0.18–0.36 km/h) [39], the eel larvae needed approximately 30–40 days to be transported from I-Lan to Je-Ju Island, which is close to the expected mean time differences between these two sites (40 days). This suggests that glass eels in Je-Ju Island were probably being transported by Kuroshio and YSWC pathways (Figure 5). The counted otolith mean ages of glass eels in Je-Ju Island, however, were only 22.9 days higher than those of glass eels in I-Lan (Table 2). The lower mean counted age differences between I-Lan and Je-Ju Island may be due to a slight underestimation of the otolith increments for glass eel samples from Je-Ju Island. The glass eels of the Geum and Yalu Rivers were located along the extensive pathway of YSWC, with expected mean ages of 90 and 150 days more than that in I-Lan, respectively (Table 2). As indicated above, the significantly lower mean counted age differences

between I-Lan and these two sites may be due to an underestimation of the otolith increments for glass eel samples. The coastal water temperature of western Korea was less than 5 °C in winter, which was unsuitable for glass eel upstream migration [31]. The glass eels that migrate to the Geum and Yalu Rivers may winter in the estuary for 1–3 months, until the water temperature rises.

A previous study has suggested that, with the western branch of the Yellow Sea Warm Current that has an eastward branch near Zhejiang waters [39] and converges with the southward Yellow Sea Coastal Current (YSCC) to form a small counterclockwise circulation current, the glass eel of Shang-Hai and Ning-Bo may possibly be transported by pathways of YSWC followed by YSCC. The tracer simulation test suggested that the Japanese eel larvae migration from spawning grounds to the east Yangtze River takes approximately 220.2 ± 10.2 days (Table 3), which is less than the estimated mean ages of glass eels in these two sites (Table 2). The dispersal of glass eel from offshore to estuaries of Shang-Hai and Ning-Bo could explain the time lag. Again, the lower mean counted age differences between estimated and counted age of glass eel samples from Shang-Hai and Ning-Bo may be due to the underestimation of the otolith increments for glass eel samples from these two sites. Interestingly, the mean estimated and counted age differences of glass eel samples from Ning-Bo were unusually high, suggesting that another possible transport distance by TSWC, which disperses glass eels from northern Taiwan to Ning-Bo, might exist. Based on the speed of TWC (0.97–1.87 km/h), if glass eels were dispersed by this path, the recruitment time differences between Wen-Zhou and Ning-Bo was about 5–10 days only, which is significantly lower than the expected time difference between them (40 days). Thus, glass eels from Shang-Hai and Ning-Bo are more likely to be transported by YSWC than TWC.

4.5. Problems of the Present Modeling Approach

The present modeling study has successfully demonstrated a considerable contribution of the transport success to the catch of *A. japonica*. However, there are some limitations to simulating the transport of *A. japonica* larvae and juvenile. This study considered only the salinity preference of this species while simulating its horizontal swimming direction, which might not be sufficient to accurately reflect the actual conditions. In addition, since this study aimed primarily to observe the transport process of this species, the potential high mortality of the larvae and juvenile was not considered [74]. On the other hand, although the JCOPE2 circulation model has been verified with observation data and showed well correspondence, the present simulation model is lack for a full-scale sensitivity analysis. For future research, more larval behavior should be investigated and applied to the simulation experiment in order to obtain a comprehensive understanding of the migration process of this species with accuracy and credibility.

5. Conclusions

The I-Lan county of Taiwan is the first recruitment place for Japanese glass eels and has the lowest mean LD and age when compared with glass eels from other sites. In general, the counted otolith age of the glass eel is proportional to the transportation distance, although with certain underestimations, especially for the later recruits. In this study, at least five main expected routes were proposed after the comprehensive analysis. These five blocks constitute the main recruitment dynamics of the Japanese eel in the East Asian Continental Shelf. Nevertheless, more sampling sites and sampling number from the same year cohorts may improve the age data resolution, which would help to better understand the dispersal mechanism of the Japanese eel larvae in East Asia Continental Shelf in detail.

Author Contributions: Y.-S.H. and H.Z. designed the experiments, analyzed the results, performed the statistical analyses, and wrote the manuscript; K.-M.H. was responsible for designing and analyzing the tracer simulation experiments, and wrote the manuscript; S.K. helped to conduct the tracer simulation experiments; L.-Y.C. and Y.I. participated in otolith age determination and manuscript writing; W.-N.T., A.S., T.Y., S.-P.H., S.-D.H. helped to collect the glass eel samples.

Funding: The authors thank National Taiwan University (105R203315, 106R203307, 107L2033-04), the Ministry of Science and Technology, Executive Yuan, Taiwan (NSC 102-2628-B-002-023-MY3, MOST 105-2313-B-002-030, MOST 106-2313-B-002-036-MY3), and the Council of Agriculture, Executive Yuan, Taiwan (106AS-11.3.4-FA-F1) for funding this project.

Acknowledgments: The authors also sincerely thank the anonymous reviewers for helping us to improve the quality of the manuscript.

Conflicts of Interest: The authors declare that they have no competing interests.

References

1. Cheng, P.W.; Tzeng, W.N. Timing of metamorphosis and estuarine arrival across the dispersal range of the Japanese eel *Anguilla japonica*. *Mar. Ecol. Prog. Ser.* **1996**, *131*, 87–96. [CrossRef]
2. Tesch, F.W.; White, R.J. *The Eel*; Wiley-Blackwell: London, UK, 2008.
3. Kuroki, M.; Aoyama, J.; Miller, M.J.; Yoshinaga, T.; Shinoda, A.; Hagihara, S.; Tsukamoto, K. Sympatric Spawning of *Anguilla marmorata* and *Anguilla japonica* in the Western North Pacific Ocean. *J. Fish Biol.* **2009**, *74*, 1853–1865. [CrossRef]
4. Han, Y.S.; Tzeng, W.N.; Liao, I.-C. Time series analysis of Taiwanese catch data of Japanese glass eels. *Zool. Stud.* **2009**, *48*, 632–639.
5. Miller, M.J.; Kimura, S.; Friedland, K.D.; Knights, B.; Kim, H.; Jellyman, D.J.; Tsukamoto, K. Review of ocean-atmospheric factors in the Atlantic and Pacific oceans influencing spawning and recruitment of anguillid eels. *Am. Fish. Soc. Symp.* **2009**, *69*, 231–249.
6. Tzeng, W.N.; Tzeng, Y.H.; Han, Y.S.; Hsu, C.C.; Chang, C.W.; Lorenzo, E.D.; Hsieh, C.H. Evaluation of multi-scale climate effects on annual recruitment levels of the Japanese eel, *Anguilla japonica*, to Taiwan. *PLoS ONE* **2012**, *7*, e30805. [CrossRef]
7. Chen, J.Z.; Huang, S.L.; Han, Y.S. Impact of long-term habitat loss on the Japanese eel *Anguilla japonica*. *Estuar. Coast. Shelf Sci.* **2014**, *151*, 361–369. [CrossRef]
8. *The 92nd Statistical Yearbook of Ministry of Agriculture, Forestry and Fisheries*; Japan Statistics Department: Tokyo, Japan, 2018.
9. Ministry of the Environment. *Red Date Book 2014, 4: Brackish-Water/Fresh-Water Fishes*; Gyosei: Tokyo, Japan, 2015. (In Japanese)
10. Jacoby, D.; Gollock, M. *Anguilla anguilla*. The IUCN Red List of Threatened Species. Version 2014.2. 2014. Available online: www.iucnredlist.org (accessed on 28 May 2013).
11. Jacoby, D.; Casselman, J.; Crook, V.; DeLucia, M.; Ahn, H.; Kaifu, K.; Kurwie, T.; Sasal, P.; Silfergrip, A.; Smith, K.; et al. Synergistic patterns of threat and the challenges facing global anguillid eel conservation. *Glob. Ecol. Conserv.* **2015**, *4*, 321–333. [CrossRef]
12. Fisheries Agency, Council of Agriculture. Executive Yuan, Taiwan. Available online: https://tesri.tesri.gov.tw/htmlarea_file/web_articles/tesri/2638/04%20the%20red%20list%20of%20freshwater%20fishes%20of%20taiwan%202017.pdf (accessed on 1 July 2017).
13. Itakura, H.; Kitagawa, T.; Miller, M.J.; Kimura, S. Declines in catches of Japanese eels in rivers and lakes across Japan: Have river and lake modifications reduced fishery catches? *Landsc. Ecol. Eng.* **2014**, *11*, 147–160. [CrossRef]
14. Itakura, H.; Kaino, T.; Miyake, Y.; Kitagawa, T.; Kimura, S. Feeding, condition and abundance of Japanese eels from natural and revetment habitats in the Tone River, Japan. *Environ. Biol. Fish.* **2015**, *98*, 1871–1888. [CrossRef]
15. Dekker, W. Did lack of spawners cause the collapse of the European eel, *Anguilla anguilla*? *Fish. Manag. Ecol.* **2003**, *10*, 365–376. [CrossRef]
16. Tanaka, E. Stock assessment of Japanese eels using Japanese abundance indices. *Fish. Sci.* **2014**, *80*, 1129–1144. [CrossRef]
17. Lin, Y.J.; Tzeng, W.N.; Han, Y.S.; Roa-Ureta, R.H. A stock assessment model for transit stock fisheries with explicit immigration and emigration dynamics: Application to upstream waves of glass eels. *Fish. Res.* **2017**, *195*, 130–140. [CrossRef]
18. Kimura, S.; Inoue, T.; Sugimoto, T. Fluctuation in the distribution of low-salinity water in the North Equatorial Current and its effect on the larval transport of the Japanese eel. *Fish. Oceanogr.* **2001**, *10*, 51–60. [CrossRef]

19. Kim, H.; Kimura, S.; Shinoda, A.; Kitagawa, T.; Sasai, Y.; Sasaki, H. Effect of El Niño on migration and larval transport of the Japanese eel (*Anguilla japonica*). *ICES J. Mar. Sci.* **2007**, *64*, 1387–1395. [CrossRef]
20. Lin, Y.F.; Wu, C.R.; Han, Y.S. A combination mode of climate variability responsible for extremely poor recruitment of the Japanese eel (*Anguilla japonica*). *Sci. Rep.* **2017**, *7*, 44469. [CrossRef]
21. Chang, Y.L.K.; Miyazawa, Y.; Béguer-Pon, M.; Han, Y.S.; Ohashi, K.; Sheng, J. Physical and biological roles of mesoscale eddies in Japanese eel larvae dispersal in the western North Pacific Ocean. *Sci. Rep.* **2018**, *8*, 5013. [CrossRef]
22. Hsiung, K.M.; Kimura, S.; Han, Y.S.; Takeshige, A.; Iizuka, Y. Effect of ENSO events on larval and juvenile duration and transport of Japanese eel (*Anguilla japonica*). *PLoS ONE* **2018**, *13*, e0195544. [CrossRef]
23. CITES. Amendments to Appendices I and II of the Convention. In Proceedings of the Conference of the Parties 14th Meeting, The Hague, The Netherlands, 3–15 June 2007.
24. Gollock, M.; Shiraishi, H.; Carrizo, S.; Crook, V.; Levy, E. *Status of Non-CITES Listed Anguillid Eels*; TRAFFIC Report; Zoological Society of London: London, UK, 2018.
25. Tsukamoto, K. Discovery of the spawning area for the Japanese eel. *Nature* **1992**, *356*, 789–791. [CrossRef]
26. Tsukamoto, K. Oceanic biology: Spawning of eels near a seamount. *Nature* **2006**, *439*, 929. [CrossRef]
27. Tsukamoto, K.; Otake, T.; Mochioka, N.; Lee, T.W.; Fricke, H.; Inagaki, T.; Aoyama, J.; Ishikawa, S.; Kimura, S.; Miller, M.J.; et al. Seamounts, new moon and eel spawning: The search for the spawning site of the Japanese eel. *Environ. Biol. Fish.* **2003**, *66*, 221–229. [CrossRef]
28. Tsukamoto, K.; Chow, S.; Otake, T.; Kurogi, H.; Mochioka, N.; Miller, M.J.; Aoyama, J.; Kimura, S.; Watanabe, S.; Yoshinaga, T.; et al. Oceanic spawning ecology of freshwater eels in the western North Pacific. *Nat. Commun.* **2011**, *2*, 179. [CrossRef]
29. Han, Y.S.; Zhang, H.; Tseng, Y.H.; Shen, M.L. Larval Japanese eel (*Anguilla japonica*) as sub-surface current bio-tracers on the East Asia continental shelf. *Fish. Oceanogr.* **2012**, *21*, 281–290. [CrossRef]
30. Han, Y.S.; Wu, C.R.; Iizuka, Y. Batch-like Arrival Waves of Glass Eels of *Anguilla japonica* in Offshore Waters of Taiwan. *Zool. Stud.* **2016**, *55*, 36.
31. Han, Y.S. Temperature-dependent recruitment delay of the Japanese glass eel *Anguilla japonica* in East Asia. *Mar. Biol.* **2011**, *158*, 2349–2358. [CrossRef]
32. McCleave, J.D.; Wippelhauser, G.S. Behavioural aspects of selective tidal stream transport in juvenile American eels. *Am. Fish. Soc. Symp.* **1987**, *1*, 138–150.
33. Nitani, H. Beginning of the Kuroshio. In *Kuroshio, Its Physical Aspects*; Stommel, H., Yoshida, K., Eds.; University of Tokyo Press: Tokyo, Japan, 1972; pp. 129–163.
34. Toole, J.M.; Millard, R.C.; Wang, Z.; Pu, S. Observations of the Pacific North Equatorial Current bifurcation at the Philippine Coast. *J. Phys. Oceanogr.* **1990**, *20*, 307–318. [CrossRef]
35. Hickox, R.; Belkin, I.; Cornillon, P.; Shan, Z. Climatology and seasonal variability of ocean fronts in the East China, Yellow and Bohai seas from satellite SST data. *Geophys. Res. Lett.* **2000**, *27*, 2945–2948. [CrossRef]
36. Ichikawa, H.; Chaen, M. Seasonal variation of heat and freshwater transports by the Kuroshio in the ECS. *J. Mar. Syst.* **2000**, *24*, 119–129. [CrossRef]
37. Su, J.L.; Yuan, Y.L. *Hydrology of Chinese Coastal Waters*; China Ocean Press: Beijing, China, 2005; p. 367. (In Chinese)
38. Chen, C.T.A. Chemical and Physical fronts in the Bohai, Yellow and East China seas. *J. Mar. Syst.* **2009**, *78*, 394–410. [CrossRef]
39. Ye, Y.C. *Marine Geo-Hazards in China*, 1st ed.; Elsevier: Amsterdam, The Netherlands, 2017; pp. 51–53.
40. Hsueh, Y.; Lie, H.J.; Ichikawa, H. On the branching of the Kuroshio west of Kyushu. *J. Geophys. Res.* **1996**, *101*, 3851–3857. [CrossRef]
41. Hsueh, Y. The Kuroshio in the East China Sea. *J. Mar. Syst.* **2000**, *24*, 131–139. [CrossRef]
42. Centurioni, L.R.; Niiler, P.P.; Lee, D.K. Observations of inflow of Philippine Sea surface water into the South China Sea through the Luzon Strait. *J. Phys. Oceanogr.* **2004**, *34*, 113–121. [CrossRef]
43. Caruso, M.J.; Gawarkiewicz, G.G.; Beardsley, R.C. Interannual variability of the Kuroshio intrusion in the South China Sea. *J. Oceanogr.* **2006**, *62*, 559–575. [CrossRef]
44. Jan, S.; Tseng, Y.H.; Dietrich, D.E. Sources of water in the Taiwan Strait. *J. Oceanogr.* **2010**, *66*, 211–221. [CrossRef]
45. Cieri, M.D.; McCleave, J.D. Discrepancies between larvae and juveniles of American eel: Is something fishy happening at metamorphosis? *J. Fish Biol.* **2000**, *57*, 1189–1198. [CrossRef]

46. Tzeng, W.N. The processes of onshore migration of the Japanese eel Anguilla japonica as revealed by otolith microstructure. In *Eel Biology*; Aida, K., Tsukamoto, K., Yamauchi, K., Eds.; Springer: Tokyo, Japan, 2003; pp. 181–190.
47. Tzeng, W.N. Relationship between growth rate and age at recruitment of *Anguilla japonica* in a Taiwan estuary as inferred from otolith growth increments. *Mar. Biol.* **1990**, *107*, 75–81. [CrossRef]
48. Shinoda, A. The Ecology of Inshore Migration of the Japanese Eel, *Anguilla japonica*. Ph.D. Thesis, University of Tokyo, Tokyo, Japan, 2004. (In Japanese).
49. Kuroki, M.; Aoyama, J.; Miller, M.J.; Wouthuyzen, S.; Arai, T.; Tsukamoto, K. Contrasting patterns of growth and migration of tropical anguillid leptocephali in the western Pacific and Indonesian Seas. *Mar. Ecol. Prog. Ser.* **2006**, *309*, 233–246. [CrossRef]
50. Yamamoto, K.; Yamauchi, K. Sexual maturation of Japanese eel and production of eel larvae in the aquarium. *Nature* **1974**, *251*, 220–222. [CrossRef]
51. Japan Aquaculture Information News. Available online: https://unaginews.blog.so-net.ne.jp/ (accessed on 21 July 2018).
52. China Eel Information News. Available online: http://www.chinaeel.cn/ (accessed on 25 March 2018).
53. Taiwan Japanese Glass Eel Reporting System. Available online: https://fad.fa.gov.tw/fafish/sys/logoutSys.htmx (accessed on 18 March 2018).
54. Mellor, G.L.; Häkkinen, S.M.; Ezer, T.; Patchen, R.C. A generalization of a sigma coordinate ocean model and an intercomparison of model vertical grids. In *Ocean Forecasting*; Springer: Berlin/Heidelberg, Germany, 2002; pp. 55–72.
55. Chang, Y.L.; Miyazawa, Y.; Béguer-Pon, M. Simulating the oceanic migration of silver Japanese eels. *PLoS ONE* **2016**, *11*, e0150187. [CrossRef]
56. Miyazawa, Y.; Zhang, R.; Guo, X.; Tamura, H.; Ambe, D.; Lee, J.S.; Okuno, A.; Yoshinari, H.; Setou, T.; Komatsu, K. Water mass variability in the western North Pacific detected in a 15-year eddy resolving ocean reanalysis. *J. Oceanogr.* **2009**, *65*, 737–756. [CrossRef]
57. Chang, Y.L.; Sheng, J.; Ohashi, K.; Béguer-Pon, M.; Miyazawa, Y. Impacts of interannual ocean circulation variability on Japanese eel larval migration in the western North Pacific Ocean. *PLoS ONE* **2015**, *10*, e0144423. [CrossRef]
58. Ishikawa, S.; Suzuki, K.; Inagaki, T.; Watanabe, S.; Kimura, Y.; Okamura, A.; Otake, T.; Mochioka, N.; Suzuki, Y.; Hasumoto, H.; et al. Spawning time and place of the Japanese eel *Anguilla japonica* in the North Equatorial Current of the western North Pacific Ocean. *Fish. Sci.* **2001**, *67*, 1097–1103. [CrossRef]
59. Shinoda, A.; Tanaka, H.; Kagawa, H.; Ohta, H.; Tsukamoto, K. Otolith microstructural analysis of reared larvae of the Japanese eel *Anguilla japonica*. *Fish. Sci.* **2004**, *70*, 339–341. [CrossRef]
60. Xu, X. A Study on Larval and Juvenile Migrations of the Japanese Eel Using a Numerical Model with Swimming Behaviors. Master's Dissertation, The University of Tokyo, Tokyo, Japan, 2015; pp. 1–50.
61. Tosi, L.; Spampanato, A.; Sola, C.; Tongiorgi, P. Relation of water odour, salinity and temperature to ascent of glass-eels, *Anguilla anguilla* (L.): A laboratory study. *J. Fish Biol.* **1990**, *36*, 327–340. [CrossRef]
62. Tabeta, O.; Tanaka, K.; Yamada, J.; Tzeng, W. Aspects of the early life history of the Japanese eel *Anguilla japonica* determined from otolith microstructure. *Nippon Suisan Gakkaishi* **1987**, *53*, 1727–1734. (In Japanese) [CrossRef]
63. McCleave, J.D. Contrasts between spawning times of *Anguilla* species estimated from larval sampling at sea and from otolith analysis of recruiting glass eels. *Mar. Biol.* **2008**, *155*, 249–262. [CrossRef]
64. Shinoda, A.; Aoyama, J.; Miller, M.J.; Otake, T.; Mochioka, N.; Watanabe, S.; Minegishi, Y.; Kuroki, M.; Yoshinaga, T.; Yokouchi, K.; et al. Evaluation of the larval distribution and migration of the Japanese eel in the western North Pacific. *Rev. Fish Biol. Fish.* **2011**, *21*, 591–611. [CrossRef]
65. Fukuda, N.; Kurogi, H.; Ambe, D.; Chow, S.; Yamamoto, T.; Yokouchi, K.; Shinoda, A.; Masuda, Y.; Sekino, M.; Saitoh, K.; et al. Location, size and age at onset of metamorphosis in the Japanese eel *Anguilla japonica*. *J. Fish Biol.* **2018**, *92*, 1342–1358. [CrossRef] [PubMed]
66. Pfeiler, E.; Toyoda, H.; Williams, M.D.; Nieman, R.A. Identification, structural analysis and function of hyaluronan in developing fish larvae (leptocephali). *Comp. Biochem. Phys. Part B Biochem. Mol. Biol.* **2002**, *132*, 443–451. [CrossRef]
67. Deibel, D.; Parrish, C.C.; Gronkjaer, P.; Munk, P.; Nielsen, T.G. Lipid class and fatty acid content of the leptocephalus larva of tropical eels. *Lipids* **2012**, *47*, 623–634. [CrossRef]

68. Tzeng, W.N.; Tsai, Y.C. Otolith microstructure and daily age of *Anguilla japonica*, Temminck & Schlegel elvers from the estuaries of Taiwan with reference to unit stock and larval migration. *J. Fish Biol.* **1992**, *40*, 845–857.
69. Umezawa, A.; Tsukamoto, K. Age and birth date of the glass eel, *Anguilla japonica*, collected in Taiwan. *Nippon Suisan Gakkaishi* **1990**, *56*, 1199–1202. [CrossRef]
70. Fukuda, N.; Kuroki, M.; Shinoda, A.; Yamada, Y.; Okamura, A.; Aoyama, J.; Tsukamoto, K. Influence of water temperature and feeding regime on otolith growth in *Anguilla japonica* glass eels and elvers: Does otolith growth cease at low temperatures? *J. Fish Biol.* **2009**, *74*, 1915–1933. [CrossRef]
71. Chang, Y.L.; Miyazawa, Y.; Béguer-Pon, M. The dynamical impact of mesoscale eddies on migration of Japanese eel larvae. *PLoS ONE* **2017**, *12*, e0172501. [CrossRef] [PubMed]
72. Bonhommeau, S.; Castonguay, M.; Rivot, E.; Richard Sabatié, R.; Le Pape, O. The duration of migration of Atlantic *Anguilla* larvae. *Fish Fish.* **2000**, *11*, 289–306. [CrossRef]
73. Lai, Y.P.; Zhou, H.; Wen, B.Y. Surface current characteristics in the Taiwan Strait observed by high-frequency radars. *IEEE J. Ocean. Eng.* **2016**, *42*, 449–457. [CrossRef]
74. Hjort, J. *Fluctuations in the Great Fisheries of Northern Europe, Viewed in the Light of Biological Research*; Rapports et Procès-Verbaux des Réunions du Conseil Permanent International Pour L'Exploration de la Mer; Andr. Fred. Høst & Fils: Copenhagen, Denmark, 1914; Volume 20, pp. 1–228.